ORGANISATION EUROPÉENNE POUR LA RECHERCHE NUCLÉAIRE

CERN PPE/92-59
16 April 1992

Search for a very light CP-odd neutral Higgs boson of the MSSM

The ALEPH Collaboration*)

Abstract

The reactions $e^+e^- \to hZ^*$ and $e^+e^- \to hA$ have been used to search for the neutral Higgs bosons h and A of the MSSM in the case where the CP-odd A is lighter than $2m_\mu$, taking into account the large $h \to AA$ decay branching ratio. No signal was found in the data sample collected until the end of 1991 by the ALEPH experiment at LEP. For $\tan\beta \geq 1$, $m_A < 2m_\mu$ is excluded at 95% CL for any m_h.

(To be submitted to Physics Letters B)

*) See next pages for the list of authors.

The ALEPH Collaboration

D. Buskulic, D. Decamp, C. Goy, J.-P. Lees, M.-N. Minard, B. Mours

Laboratoire de Physique des Particules (LAPP), IN²P³-CNRS, 74019 Annecy-le-Vieux Cedex, France

R. Alemany, F. Ariztizabal, P. Comas, J.M. Crespo, M. Delfino, E. Fernandez, V. Gaitan, Ll. Garrido, Ll.M. Mir, A. Pacheco, A. Pascual

Institut de Fisica d'Altes Energies, Universitat Autonoma de Barcelona, 08193 Bellaterra (Barcelona), Spain[8]

D. Creanza, M. de Palma, A. Farilla, G. Iaselli, G. Maggi, M. Maggi, S. Natali, S. Nuzzo, M. Quattromini, A. Ranieri, G. Raso, F. Romano, F. Ruggieri, G. Selvaggi, L. Silvestris, P. Tempesta, G. Zito

INFN Sezione di Bari e Dipartimento di Fisica dell' Università, 70126 Bari, Italy

Y. Gao, H. Hu,[21] D. Huang, X. Huang, J. Lin, J. Lou, C. Qiao,[21] T. Wang, Y. Xie, D. Xu, R. Xu, J. Zhang, W. Zhao

Institute of High-Energy Physics, Academia Sinica, Beijing, The People's Republic of China[9]

W.B. Atwood,[2] L.A.T. Bauerdick,[26] E. Blucher, G. Bonvicini, F. Bossi, J. Boudreau, T.H. Burnett,[3] H. Drevermann, R.W. Forty, R. Hagelberg, J. Harvey, S. Haywood, J. Hilgart, R. Jacobsen, B. Jost, J. Knobloch, E. Lançon, I. Lehraus, T. Lohse, A. Lusiani, M. Martinez, P. Mato, T. Mattison, H. Meinhard, S. Menary,[27] T. Meyer, A. Minten, A. Miotto, R. Miquel, H.-G. Moser, J. Nash, P. Palazzi, J.A. Perlas, F. Ranjard, G. Redlinger, L. Rolandi,[28] A. Roth,[30] J. Rothberg,[3] T. Ruan,[21,33] M. Saich, D. Schlatter, M. Schmelling, F. Sefkow, W. Tejessy, H. Wachsmuth, W. Wiedenmann, T. Wildish, W. Witzeling, J. Wotschack

European Laboratory for Particle Physics (CERN), 1211 Geneva 23, Switzerland

Z. Ajaltouni, F. Badaud, M. Bardadin-Otwinowska, A.M. Bencheikh, R. El Fellous, A. Falvard, P. Gay, C. Guicheney, P. Henrard, J. Jousset, B. Michel, J-C. Montret, D. Pallin, P. Perret, B. Pietrzyk, J. Proriol, F. Prulhière, G. Stimpfl

Laboratoire de Physique Corpusculaire, Université Blaise Pascal, IN²P³-CNRS, Clermont-Ferrand, 63177 Aubière, France

T. Fearnley, J.D. Hansen, J.R. Hansen, P.H. Hansen, R. Møllerud, B.S. Nilsson

Niels Bohr Institute, 2100 Copenhagen, Denmark[10]

I. Efthymiopoulos, A. Kyriakis, E. Simopoulou, A. Vayaki,[1] K. Zachariadou

Nuclear Research Center Demokritos (NRCD), Athens, Greece

J. Badier, A. Blondel, G. Bonneaud, J.C. Brient, G. Fouque, A. Gamess, S. Orteu, A. Rosowsky, A. Rougé, M. Rumpf, R. Tanaka, H. Videau

Laboratoire de Physique Nucléaire et des Hautes Energies, Ecole Polytechnique, IN²P³-CNRS, 91128 Palaiseau Cedex, France

D.J. Candlin, M.I. Parsons, E. Veitch

Department of Physics, University of Edinburgh, Edinburgh EH9 3JZ, United Kingdom[11]

L. Moneta, G. Parrini

Dipartimento di Fisica, Università di Firenze, INFN Sezione di Firenze, 50125 Firenze, Italy

M. Corden, C. Georgiopoulos, M. Ikeda, J. Lannutti, D. Levinthal,[16] M. Mermikides†, L. Sawyer, S. Wasserbaech

Supercomputer Computations Research Institute and Dept. of Physics, Florida State University, Tallahassee, FL 32306, USA [13,14,15]

A. Antonelli, R. Baldini, G. Bencivenni, G. Bologna,[5] P. Campana, G. Capon, F. Cerutti, V. Chiarella, B. D'Ettorre-Piazzoli,[32] G. Felici, P. Laurelli, G. Mannocchi,[6] F. Murtas, G.P. Murtas, L. Passalacqua, M. Pepe-Altarelli, P. Picchi[5]

Laboratori Nazionali dell'INFN (LNF-INFN), 00044 Frascati, Italy

B. Altoon, O. Boyle, P. Colrain, I. ten Have, J.G. Lynch, W. Maitland, W.T. Morton, C. Raine, J.M. Scarr, K. Smith, A.S. Thompson, R.M. Turnbull

Department of Physics and Astronomy, University of Glasgow, Glasgow G12 8QQ,United Kingdom[11]

B. Brandl, O. Braun, R. Geiges, C. Geweniger, P. Hanke, V. Hepp, E.E. Kluge, Y. Maumary, A. Putzer, B. Rensch, A. Stahl, K. Tittel, M. Wunsch

Institut für Hochenergiephysik, Universität Heidelberg, 6900 Heidelberg, Fed. Rep. of Germany[17]

A.T. Belk, R. Beuselinck, D.M. Binnie, W. Cameron, M. Cattaneo, D.J. Colling, P.J. Dornan,[1] S. Dugeay, A.M. Greene, J.F. Hassard, N.M. Lieske, S.J. Patton, D.G. Payne, M.J. Phillips, J.K. Sedgbeer, I.R. Tomalin, A.G. Wright

Department of Physics, Imperial College, London SW7 2BZ, United Kingdom[11]

P. Girtler, D. Kuhn, G. Rudolph

Institut für Experimentalphysik, Universität Innsbruck, 6020 Innsbruck, Austria[19]

C.K. Bowdery, T.J. Brodbeck, A.J. Finch, F. Foster, G. Hughes, D. Jackson, N.R. Keemer, M. Nuttall, A. Patel, T. Sloan, S.W. Snow, E.P. Whelan

Department of Physics, University of Lancaster, Lancaster LA1 4YB, United Kingdom[11]

T. Barczewski, K. Kleinknecht, J. Raab, B. Renk, S. Roehn, H.-G. Sander, H. Schmidt, F. Steeg, S.M. Walther, B. Wolf

Institut für Physik, Universität Mainz, 6500 Mainz, Fed. Rep. of Germany[17]

J-J. Aubert, C. Benchouk, V. Bernard, A. Bonissent, J. Carr, P. Coyle, J. Drinkard, F. Etienne, S. Papalexiou, P. Payre, Z. Qian, D. Rousseau, P. Schwemling, M. Talby

Centre de Physique des Particules, Faculté des Sciences de Luminy, IN²P³-CNRS, 13288 Marseille, France

S. Adlung, H. Becker, W. Blum,[1] D. Brown, P. Cattaneo,[29] G. Cowan, B. Dehning, H. Dietl, F. Dydak,[25] M. Fernandez-Bosman, M. Frank, A.W. Halley, T. Hansl-Kozanecka,[2,22] J. Lauber, G. Lütjens, G. Lutz, W. Männer, Y. Pan, R. Richter, H. Rotscheidt, J. Schröder, A.S. Schwarz, R. Settles, U. Stierlin, U. Stiegler, R. St. Denis, M. Takashima,[4] J. Thomas,[4] G. Wolf

Max-Planck-Institut für Physik und Astrophysik, Werner-Heisenberg-Institut für Physik, 8000 München, Fed. Rep. of Germany[17]

V. Bertin, J. Boucrot, O. Callot, X. Chen, A. Cordier, M. Davier, J.-F. Grivaz, Ph. Heusse, P. Janot, D.W. Kim,[20] F. Le Diberder, J. Lefrançois,[1] A.-M. Lutz, M.-H. Schune, J.-J. Veillet, I. Videau, Z. Zhang, F. Zomer

Laboratoire de l'Accélérateur Linéaire, Université de Paris-Sud, IN²P³-CNRS, 91405 Orsay Cedex, France

D. Abbaneo, S.R. Amendolia, G. Bagliesi, G. Batignani, L. Bosisio, U. Bottigli, C. Bradaschia, M. Carpinelli, M.A. Ciocci, R. Dell'Orso, I. Ferrante, F. Fidecaro,[1] L. Foà, E. Focardi, F. Forti, A. Giassi, M.A. Giorgi, F. Ligabue, E.B. Mannelli, P.S. Marrocchesi, A. Messineo, F. Palla, G. Rizzo, G. Sanguinetti, J. Steinberger, R. Tenchini, G. Tonelli, G. Triggiani, C. Vannini, A. Venturi, P.G. Verdini, J. Walsh

Dipartimento di Fisica dell'Università, INFN Sezione di Pisa, e Scuola Normale Superiore, 56010 Pisa, Italy

J.M. Carter, M.G. Green, P.V. March, T. Medcalf, I.S. Quazi, J.A. Strong, L.R. West

Department of Physics, Royal Holloway & Bedford New College, University of London, Surrey TW20 OEX, United Kingdom[11]

D.R. Botterill, R.W. Clifft, T.R. Edgecock, M. Edwards, S.M. Fisher, T.J. Jones, P.R. Norton, D.P. Salmon, J.C. Thompson

Particle Physics Dept., Rutherford Appleton Laboratory, Chilton, Didcot, Oxon OX11 OQX, United Kingdom[11]

B. Bloch-Devaux, P. Colas, W. Kozanecki,[2] M.C. Lemaire, E. Locci, S. Loucatos, E. Monnier, P. Perez, F. Perrier, J. Rander, J.-F. Renardy, A. Roussarie, J.-P. Schuller, J. Schwindling, D. Si Mohand, B. Vallage

Service de Physique des Particules, DAPNIA, CE-Saclay, 91191 Gif-sur-Yvette Cedex, France[18]

R.P. Johnson, A.M. Litke, G. Taylor, J. Wear

Institute for Particle Physics, University of California at Santa Cruz, Santa Cruz, CA 95064, USA[36]

J.G. Ashman, W. Babbage, C.N. Booth, C. Buttar, R.E. Carney, S. Cartwright, F. Combley, F. Hatfield, P. Reeves, L.F. Thompson

Department of Physics, University of Sheffield, Sheffield S3 7RH, United Kingdom[11]

E. Barberio, S. Brandt, C. Grupen, L. Mirabito,[31] U. Schäfer, H. Seyerd

Fachbereich Physik, Universität Siegen, 5900 Siegen, Fed. Rep. of Germany[17]

G. Ganis,[35] G. Giannini, B. Gobbo, F. Ragusa[24]

Dipartimento di Fisica, Università di Trieste e INFN Sezione di Trieste, 34127 Trieste, Italy

L. Bellantoni, D. Cinabro,[34] J.S. Conway, D.F. Cowen,[23] Z. Feng, D.P.S. Ferguson, Y.S. Gao, J. Grahl, J.L. Harton, R.C. Jared,[7] B.W. LeClaire, C. Lishka, Y.B. Pan, J.R. Pater, Y. Saadi, V. Sharma, M. Schmitt, Z.H. Shi, Y.H. Tang, A.M. Walsh, F.V. Weber, M.H. Whitney, Sau Lan Wu, X. Wu, G. Zobernig

Department of Physics, University of Wisconsin, Madison, WI 53706, USA[12]

---

†Deceased.
[1]Now at CERN, PPE Division, 1211 Geneva 23, Switzerland.
[2]Permanent adddress: SLAC, Stanford, CA 94309, USA.
[3]Permanent address: University of Washington, Seattle, WA 98195, USA.
[4]Now at SSCL, Dallas, TX, U.S.A.
[5]Also Istituto di Fisica Generale, Università di Torino, Torino, Italy.
[6]Also Istituto di Cosmo-Geofisica del C.N.R., Torino, Italy.
[7]Permanent address: LBL, Berkeley, CA 94720, USA.
[8]Supported by CICYT, Spain.
[9]Supported by the National Science Foundation of China.
[10]Supported by the Danish Natural Science Research Council.
[11]Supported by the UK Science and Engineering Research Council.
[12]Supported by the US Department of Energy, contract DE-AC02-76ER00881.
[13]Supported by the US Department of Energy, contract DE-FG05-87ER40319.
[14]Supported by the NSF, contract PHY-8451274.
[15]Supported by the US Department of Energy, contract DE-FC0S-85ER250000.
[16]Supported by SLOAN fellowship, contract BR 2703.
[17]Supported by the Bundesministerium für Forschung und Technologie, Fed. Rep. of Germany.
[18]Supported by the Direction des Sciences de la Matière, C.E.A.
[19]Supported by Fonds zur Förderung der wissenschaftlichen Forschung, Austria.
[20]Supported by the Korean Science and Engineering Foundation and Ministry of Education.
[21]Supported by the World Laboratory.
[22]On leave of absence from MIT, Cambridge, MA 02139, USA.
[23]Now at California Institute of Technology, Pasadena, CA 91125, USA.
[24]Now at Dipartimento di Fisica, Università di Milano, Milano, Italy.
[25]Also at CERN, PPE Division, 1211 Geneva 23, Switzerland.
[26]Now at DESY, Hamburg, Germany.
[27]Now at University of California at Santa Barbara, Santa Barbara, CA 93106, USA.
[28]Also at Dipartimento di Fisica, Università di Trieste, Trieste, Italy.
[29]Now at INFN, Pavia, Italy.
[30]Now at Lufthansa, Hamburg, Germany.
[31]Now at Institut de Physique Nucléaire de Lyon, 69622 Villeurbanne, France.
[32]Also at Università di Napoli, Dipartimento di Scienze Fisiche, Napoli, Italy.
[33]On leave of absence from IHEP, Beijing, The People's Republic of China.
[34]Now at Harvard University, Cambridge, MA 02138, U.S.A.
[35]Supported by the Consorzio per lo Sviluppo dell'Area di Ricerca, Trieste, Italy.
[36]Supported by the US Department of Energy, grant DE-FG03-92ER40689.

1. Introduction.

The mass matrix of the CP-even neutral Higgs bosons of the MSSM (the minimal supersymmetric extension of the standard model) is affected by radiative corrections[1] which are substantial enough, given the large value of the top-quark mass, to upset the familiar mass relations[2] obtained at the tree level. In particular, the relation $m_A > m_h$ between the masses of the CP-odd A and of h, the lighter of the CP-even Higgs bosons, no longer holds in most of the region of the MSSM parameter space relevant in Z decays, and the new decay mode $h \rightarrow AA$ has to be taken into account when $m_A < m_h/2$. This configuration has been investigated in detail by the ALEPH Collaboration[3,4] except, as explained in Ref. 4, when $m_A < 2m_\mu$.

The analysis reported here completes the search for the neutral Higgs bosons h and A of the MSSM in Z decays *via* the processes $Z \rightarrow hZ^*$ and $Z \rightarrow hA$, in the specific case $m_A < 2m_\mu$. In Section 2, the decay characteristics of such a very light A boson are indicated. In Sections 3 and 4, the results of previously published analyses are applied to the two Z decay processes under investigation, and constraints are obtained which exclude a long-lived A boson. In Section 5, new analyses are presented, specifically aimed at the complementary configuration in which the A boson is short-lived.

As suggested by the large ratio of the top to the bottom-quark masses and as required in the MSSM, at least in its version involving the smallest set of parameters,[5] $\tan\beta \geq 1$ is systematically assumed in the following ($\tan\beta$ is the ratio of the vacuum expectation values developed by the two Higgs doublets). To simplify the presentation, the discussion in Sections 3 to 5 is detailed using a typical set of parameters in the calculation of the radiative corrections, namely a top-quark mass m_t of 140 GeV/c^2 and a mass $m_{\tilde{t}}$ of 1 TeV/c^2 for its supersymmetric partners, assumed to be mass degenerate. The analysis is however extended in Section 6, and the results obtained for the above typical set of parameters are shown to be generally valid.

In the following, all limits or excluded domains are given at the 95% confidence level.

2. Decay characteristics of a very light A.

For $m_A < 2m_\mu$, the only A decay modes are $A \rightarrow e^+e^-$, which takes place at the tree level, and $A \rightarrow \gamma\gamma$, which proceeds through loops. In contrast to the $h \rightarrow \gamma\gamma$ decay, these loops involve only quarks, charged leptons and charginos, the supersymmetric partners of the W and of the charged Higgs bosons. The formulae for the various amplitudes can be found in Appendix C of Ref. 2 and have been used to calculate the A lifetime and its decay branching ratios.

For convenience, the A lifetime is expressed in the following as a mean decay length per GeV/c and is denoted λ_A. Multiplying λ_A by the A laboratory momentum gives the A mean decay length, which is the quantity directly relevant for its observability within a given detector. As an example, Fig. 1 shows λ_A and $B_{\gamma\gamma}$, the A decay branching ratio

into $\gamma\gamma$, as a function of m_A for $\tan\beta = 1$, 2 and 10. Since the chargino masses and field contents are *a priori* unknown, all the parameters of the MSSM have been varied, imposing only that the lighter chargino mass exceed its present lower limit[4] of 45 GeV/c^2. The dashed and dotted curves in Fig. 1 correspond to the maximally destructive and maximally constructive chargino contributions thus obtained, while the full curves correspond to negligible chargino contributions.

It can be seen that, depending on m_A and on $\tan\beta$, both λ_A and $B_{\gamma\gamma}$ can vary widely. Therefore, these will be simply considered as free parameters in the following while the precise value of m_A between 0 and $2m_\mu$ is irrelevant in practice.

3. Results inferred from previous studies, applied to the reaction $e^+e^- \to hZ^*$.

For $m_A \sim 0$ and once the amount of radiative correction in the CP-even sector is fixed, only one free parameter remains in addition to λ_A and $B_{\gamma\gamma}$. In particular, there is a one-to-one correspondence between m_h and $\tan\beta$, as shown in Fig. 2a, or between m_h and α, the mixing angle in the CP-even sector. The maximum h mass is obtained for $\tan\beta = 1$ and its value, for the typical set of m_t and $m_{\tilde{t}}$ chosen, is 48 GeV/c^2.

Although $h \to AA$ is the dominant h decay mode when it is kinematically allowed, there remains some room for other possibilities. Indeed, the hAA coupling even vanishes at tree level for $\tan\beta = 1$, but this does not remain the case when the recently calculated[6] radiative corrections to the hAA vertex are taken into account. The $h \to AA$ decay branching ratio, B_{AA}, is shown in Fig. 2b as a function of m_h.

The standard model Higgs boson searches reported in Ref. 4 can be applied to the reaction $e^+e^- \to hZ^*$ when h does not decay into AA by simply multiplying the numbers of events expected (given in Tables 5.2 and 5.3 of Ref. 4) by the production cross-section reduction factor $\sin^2(\beta-\alpha)$ and by $(1 - B_{AA})$. This assumes that the search efficiencies are the same for a standard model Higgs boson and for h, when h does not decay to AA. It is indeed the case as the relative fractions of decays into hadrons and into τ-pairs are very similar (when $\tan\beta \geq 1$), and because of the highly inclusive nature of the searches performed.

The result is shown in Fig. 2c. It can be seen that the h mass range from 10 to 28 GeV/c^2 is excluded.

4. Results inferred from previous studies, applied to the reaction $e^+e^- \to hA$.

4.1 *Contribution to the Z width.*

For a very light A, the contribution of hA pair production to the Z width reads:

$$\Gamma(Z \to hA) = \frac{1}{2}\cos^2(\beta-\alpha)\Gamma_{\nu\bar{\nu}}\left(1 - \frac{{m_h}^2}{{m_Z}^2}\right)^3 .$$

Since any non-standard contribution to the Z width is restricted[4] to less than 0.28 $\Gamma_{\nu\bar{\nu}}$, irrespective of the final state topology, it follows that m_h must exceed 20 GeV/c^2. This overlaps with the previous result, thus excluding any m_h below 28 GeV/c^2.

4.2 *Direct searches.*

When h does not decay into AA and when the A lifetime is sufficiently large for it to escape the detector, the hA final state is very similar to the one resulting from the production of a standard model Higgs boson H in the reaction $e^+e^- \rightarrow HZ^*$ with $Z^* \rightarrow \nu\bar{\nu}$. The analysis performed in the latter case[4] can therefore be used again in the present configuration.

The procedure is the following. For a given h mass, the hA production cross-section and $(1 - B_{AA})$ are calculated. The search efficiency is again taken from Tables 5.2 and 5.3 of Ref. 4 (the energy spectra of H in $Z \rightarrow HZ^*$ and of h in $Z \rightarrow hA$, with $m_A \sim 0$, are in fact different, but it has been checked that this way of estimating the search efficiency is indeed conservative). A predicted number of events is then obtained, which applies in the case of a very long-lived, invisible A. Given the size of the ALEPH detector, this result is finally translated into an upper limit on λ_A, the A momentum being fixed by m_h.

The result is shown in Fig. 3 as a function of m_h. For any value of m_h, a very long-lived A boson is excluded: the only mean decay lengths per GeV/c which remain allowed are shorter than a few cm/(GeV/c).

5. Analysis of the reaction $e^+e^- \rightarrow hA$ with $h \rightarrow AA$.

5.1 *Introduction.*

It is apparent from the curves shown in Fig. 1 that the AAA final state may show up in three different ways: *i)* for A lifetimes large enough for most of the A bosons produced to escape the detector before decaying, as a purely invisible final state, *ii)* for smaller A lifetimes, as one or two visible low mass systems with missing energy , *iii)* for even smaller A lifetimes, as three visible low mass systems. Each of these low mass systems may consist either of an e^+e^- pair, possibly with a vertex detached from the interaction point, or of two photons, usually unresolved in the ALEPH electromagnetic calorimeter (ECAL) for such energetic very light A bosons.

A specific analysis has been developed to search for the totally and partly visible final states. It has been applied to the data sample collected in 1991 by the ALEPH experiment at LEP corresponding to $\sim$ 300 000 hadronic Z decays. In this sample, all major components of the detector[7] were required to be simultaneously operational and all major trigger logics enabled (for the present analysis, the most relevant trigger is the "total energy trigger" which requires an ECAL energy of at least 6.5 GeV in the barrel or of at least 3.8 GeV in either endcap).

5.2 *Selection.*

For the events containing reconstructed charged tracks, it is required that two of them at least be "good tracks" or belong to a "good V^0" (a V^0 is a long-lived neutral particle decaying into two charged particles within the tracking volume). A good track must have four coordinates or more in the TPC and must originate from a cylinder of radius 2.5 cm and of length 14 cm, coaxial with the beam and centered at the nominal interaction point. The direction of a good V^0 must approach the nominal interaction point within the same tolerance as a good charged track, and both of the tracks forming a good V^0 must have at least four TPC coordinates. In addition, these events should not contain any good track nor any track from a good V^0 with $|\cos\theta| > 0.95$. Here and in the following, θ designates a polar angle, measured with respect to the beam axis.

For the purely neutral events, the following conditions are required:

i) The event time, determined using the multiple sampling of the ECAL signals during their rise time, must be within 100 ns from the beam crossing time.

ii) The event must contain photons, identified in the ECAL using the characteristic longitudinal and transverse developments of electromagnetic showers. The total energy of these photons must exceed 10 GeV.

iii) The energy weighted mean of the distances of closest approach to the nominal interaction point of the lines of flight of these photons must not exceed 50 cm in the plane transverse to the beam axis and 80 cm along that axis. The photon lines of flights are reconstructed thanks to the transverse and longitudinal granularity of the ECAL.

iv) The total energy collected within $|\cos\theta| > 0.95$ must be smaller than 5 GeV.

v) Not more than one charged track should be reconstructed with at least six ITC but no TPC coordinates. The inner tracking chamber (ITC) covers a solid angle larger than the TPC and provides up to eight track coordinates.

The first three criteria are designed to reject cosmic ray events while the last two criteria efficiently reject the events from Bhabha scattering at low angle with respect to the beam axis.

For all the events remaining at this stage, the charged and neutral particles are clustered into jets, using the JADE algorithm[8] with a y_{cut} value of 10^{-4} corresponding to a maximum jet mass of 0.9 GeV/c^2. Only one, two and three-jet events are kept, provided that each jet contains either no track or exactly two oppositely charged tracks (good or from a good V^0). For two and three-jet events, it is required that all jet directions satisfy $|\cos\theta| < 0.95$, while for single-jet events, the jet direction should fulfill $|\cos\theta| < 0.75$. In all cases, not more than 1 GeV should be collected within 12° of the beam axis.

In three-jet events, the missing energy is required to be smaller than 10 GeV. In addition, no jet-jet angle should exceed 165°. This last cut removes the bulk of the

irreducible background from the reaction $e^+e^- \to \gamma\gamma\gamma$ in which one of the three final state photons tends to have a low energy, thus rendering almost collinear the pair formed with the other two photons. This leads to 3 events in the data while 5.4 are expected from the reaction $e^+e^- \to \gamma\gamma\gamma$.

For two-jet events also, the acollinearity angle should be smaller than 165°. In addition, the acoplanarity angle should not exceed 175°, and the component of the missing momentum transverse to the beam axis should be larger than 5 GeV/c unless the event total visible mass exceeds 25 GeV/c^2. These cuts are designed to remove the three-photon events in which one of the photons escapes undetected in the beam pipe, and to reduce the background from low multiplicity hadronic events, in particular from $\gamma\gamma$ interactions, to a level of less than one event expected . No two-jet events remain in the data.

In single-jet events, the component of the jet momentum transverse to the beam is required to exceed 10 GeV/c, which removes the large background from those radiative lepton pairs in which the leptons are emitted at low polar angle and remain undetected. Two events survive in the data, in good agreement with the expectation from the reaction $e^+e^- \to \nu\bar{\nu}\gamma$.

Altogether, this selection therefore leads to five candidate events.

5.3 *Selection efficiency.*

The selection efficiency depends on m_h, on λ_A and on $B_{\gamma\gamma}$.

A full simulation of the signal process has been performed for two representative sets of parameters: *i)* $m_h = 33$ GeV/c^2, $\lambda_A = 1$ cm/(GeV/c) and $B_{\gamma\gamma} = 55\%$; *ii)* $m_h = 44$ GeV/c^2, $\lambda_A = 20$ cm/(GeV/c) and $B_{\gamma\gamma} = 20\%$. The efficiencies obtained are 49% and 36%, respectively. A simplified simulation has been used to extrapolate those results to other values of the parameters. The features included in this simplified simulation are: the trigger conditions, the geometrical acceptance, the track reconstruction efficiency and the selection cuts. The simplified simulation reproduces not only the overall efficiencies, but also the charged track and jet multiplicities resulting from the analysis applied to the fully simulated samples. As can be expected, the most sensitive parameter is λ_A since the efficiency vanishes when the typical decay length becomes much larger than the size of the detector.

Examples of efficiencies as a function of λ_A are shown in Fig. 4. For $m_h > 28$ GeV/c^2 and $\lambda_A < 10$ cm/(GeV/c), efficiencies in excess of $\sim 30\%$ are systematically obtained. Because of the jet-jet angle cut, the efficiency for $\lambda_A = 0$ decreases for smaller m_h, and vanishes for $m_h < 13$ GeV/c^2.

5.4 *Results.*

For any value of the h mass, the hA production cross-section and the branching ratio of h into AA are computed. The number of events in the AAA final state expected to be

detected is then obtained as a function of λ_A, using the selection efficiency determined as indicated above (for a given value of λ_A, the value of $B_{\gamma\gamma}$ which is used is the one which leads to the lowest efficiency). Given the observation of 5 candidate events, a lower limit on λ_A results, always in excess of $\sim$ 10 m. For $m_h < 13$ GeV/c^2 however, this analysis does not exclude λ_A values smaller than $\sim$ 1.5 cm. These results are shown in Fig. 3.

Since, for any $m_h > 13$ GeV/c^2, the lower limit on λ_A obtained here conflicts with the upper limit obtained in Section 4.2, all of the h mass range from 13 GeV/c^2 up to the maximum theoretically allowed value of 48 GeV/c^2 is excluded.

Combining this with the results obtained in Sections 3 and 4.1 which exclude $m_h <$ 28 GeV/c^2, it can be seen that no h mass values remain allowed and, therefore, that a very light CP-odd A boson is excluded, irrespective of its lifetime, of its decay branching ratio into $\gamma\gamma$, and of m_h or $\tan\beta$.

6. What if the radiative correction is varied ?

Up to now, all the analysis has been conducted for typical values of m_t and $m_{\tilde{t}}$, namely $m_t = 140$ GeV/c^2 and $m_{\tilde{t}} = 1$ TeV/c^2. In fact, these quantities contribute only through the specific combination

$$\varepsilon_0 = \frac{3g^2}{8\pi^2}\frac{m_t^4}{m_W^2}\log\left(\frac{m_{\tilde{t}}^2}{m_t^2}\right)$$

which can be chosen as the single parameter controlling the amount of radiative correction in the CP-even Higgs sector. This however necessitates the additional assumption that the mass splitting among the two supersymmetric partners of the top quark is small, compared to their average mass. This simplifying assumption will be maintained in the following discussion.

As stated earlier, for $m_A \sim 0$ and $\tan\beta \geq 1$, there is a maximum value for m_h, reached when $\tan\beta = 1$ and denoted m_{lim}. This value is uniquely related to ε_0 as shown in Fig. 5. For the typical values of m_t and $m_{\tilde{t}}$ above, $\varepsilon_0 = (62$ GeV/$c^2)^2$ and $m_{lim} =$ 48 GeV/c^2. When ε_0 becomes increasingly large, m_{lim} quickly approaches its asymptotic value of 64 GeV/c^2 (it has been checked that scalar top mass splitting does not modify this value).

For the typical set of m_t and $m_{\tilde{t}}$ chosen, four methods have been used to exclude all of the theoretically allowed h mass range. They are briefly recalled here:

i) Too large a contribution of $Z \rightarrow hA$ to the Z width excludes the lowest h mass range, up to $m_1 = 20$ GeV/c^2. (Section 4.1)

ii) The searches for the standard model Higgs boson, applied to $e^+e^- \rightarrow hZ^*$ with h not decaying into AA, exclude the h mass range from $m_2 = 10$ GeV/c^2 to $m_3 = 28$ GeV/c^2. (Section 3)

iii) The techniques developed to search for the standard model Higgs boson in the $H\nu\bar{\nu}$

final state can be used to search for the hA final state when h does not decay into AA and when A escapes undetected. An upper limit on the A lifetime, as a function of m_h, is thus set for any $m_h < m_{lim}$. (Section 4.2)

iv) Direct searches are performed for the hA final state when h does decay into an A pair. A lower limit on the A lifetime, as a function of m_h, is thus set for 13 GeV/c^2 < $m_h < m_{lim}$. The h mass range in which the A lifetime lower limit is larger than the upper limit obtained in *iii)* extends from 13 GeV/c^2 to $m_4 = m_{lim}$. This mass range is therefore excluded. (Section 5)

When ε_0 is varied, the limiting values m_1, m_2, m_3 and m_4 evolve and define excluded domains in the (ε_0, m_h) plane as indicated in Fig. 5. The steps shown by m_2 are due to the rapid variations of B_{AA} at the $D\bar{D}$ and $B\bar{B}$ thresholds. It can be seen that any $m_h < m_{lim}$ is excluded by at least one of the above methods, whatever the value taken by ε_0, except for a small m_h region between m_1 and the $D\bar{D}$ threshold, when (6 GeV/c^2)^2 < ε_0 < (10 GeV/c^2)^2.

In this particular region, method *ii)* fails because B_{AA} is close to unity and, at the same time, the cross-section for $e^+e^- \rightarrow hZ^*$ is strongly reduced with respect to the corresponding one in the minimal standard model. The process $e^+e^- \rightarrow hA$, on the other hand, has a much larger cross-section, and method *iii)* still provides an upper limit on λ_A of 8 cm/(GeV/c). To obtain a lower limit on λ_A, the reaction $e^+e^- \rightarrow h\nu\bar{\nu}$ with $h \rightarrow AA$ can be used: unless it is invisible, the final state consists of one or two energetic low mass systems and the analysis of Section 5 is therefore applicable. It leads to a lower limit on λ_A of a few meters/(GeV/c), thus excluding this small region too.

7. Conclusion.

Using a large variety of methods, it has been possible to exclude, for $\tan\beta \geq 1$, a CP-odd A Higgs boson of the MSSM with a mass below the two-muon threshold. The result obtained is valid irrespective of the size of the radiative corrections in the CP-even sector.

Acknowledgements.

We wish to thank our colleagues from the accelerator divisions for the operation of LEP. We are indebted to the engineers and technicians in all our institutions for their contribution to the good performance of ALEPH. Those of us from non-member countries thank CERN for its hospitality.

References.

1. For a complete set of formulae and for references to earlier work, see:
   J. Ellis, G. Ridolfi and F. Zwirner, Phys. Lett. **262B** (1991) 477.
2. J.F. Gunion, H.E. Haber, G. L. Kane and S. Dawson,
   "The Higgs Hunter's Guide" (Addison Wesley, 1990).
3. D. Decamp et al., (ALEPH Coll.), Phys. Lett. **265B** (1991) 475.
4. D. Decamp et al., (ALEPH Coll.), "Searches for New Particles in Z Decays Using the ALEPH Detector", CERN-PPE/91-149, 20 September 1991, submitted to Physics Reports.
5. See for instance:
   F. Zwirner, "The quest for low-energy supersymmetry and the role of high-energy e^+e^- colliders", CERN-TH.6357/91, December 1991, to appear in the Proceedings of the Workshop on Physics and Experiments with Linear Colliders, Saariselkä, Finland, 9-14 September 1991.
6. A. Brignole et al., Phys. Lett. **271B** (1991) 123.
7. D. Decamp et al., (ALEPH Coll.), Nucl. Instr. Meth. **A294** (1990) 121.
8. S. Bethke et al., (JADE Coll.), Phys. Lett. **213B** (1988) 235.

Figure Captions.

1. For $m_A < 2m_\mu$, and as a function of m_A: the branching ratio $B_{\gamma\gamma}$ of A into $\gamma\gamma$ and λ_A, the A mean decay length per GeV/c, for $\tan\beta$= 1, 2 and 10. Note the different vertical scales in the three λ_A plots. The full curves are obtained neglecting any chargino contribution to the $A \to \gamma\gamma$ decay amplitude while the dashed and dotted curves correspond to maximally destructive and maximally constructive chargino contributions, respectively.

2. For $m_A < 2m_\mu$ and as a function of m_h:
a) $\tan\beta$;
b) the branching ratio B_{AA} of h into AA;
c) the number of events from $e^+e^- \to hZ^*$, with h not decaying into AA, expected to be found in the searches for the standard model Higgs boson reported in Ref. 4.
The typical set of parameters $m_t = 140$ GeV/c^2 and $m_{\tilde{t}} = 1$ TeV/c^2 is chosen, and negligible scalar top mass splitting is assumed.

3. As a function of m_h:
(A) upper limit on λ_A;
(B) lower limit on λ_A (for $m_h > 13$ GeV/c^2) or excluded λ_A range (for $m_h < 13$ GeV/c^2).
The typical set of parameters $m_t = 140$ GeV/c^2 and $m_{\tilde{t}} = 1$ TeV/c^2 is chosen, and negligible scalar top mass splitting is assumed.

4. For $m_h = 44$ GeV/c^2 and $h \to AA$, efficiencies of the searches for the various final states arising from the reaction $e^+e^- \to hA$, as a function of λ_A: all final states combined (full line); three jets (dashed); two jets (dotted); single jets (dash-dotted).

5. In the (ε_0, m_h) plane, domains excluded by:
(A) the Z width, below m_1;
(B) the searches in the reaction $e^+e^- \to hZ^*$, from m_2 to m_3;
(C) the searches in the reaction $e^+e^- \to hA$, from 13 GeV/c^2 to m_4.
The grey area, above m_{lim}, is excluded by the theory (with $\tan\beta \geq 1$). Negligible scalar top mass splitting is assumed. The vertical line corresponds to the typical values m_t = 140 GeV/c^2 and $m_{\tilde{t}} = 1$ TeV/c^2. The top quark mass values given in the upper scale are deduced from the corresponding ε_0 values in the lower scale, assuming a constant $m_{\tilde{t}}/m_t$ ratio equal to (1 TeV/c^2)/(140 GeV/c^2).

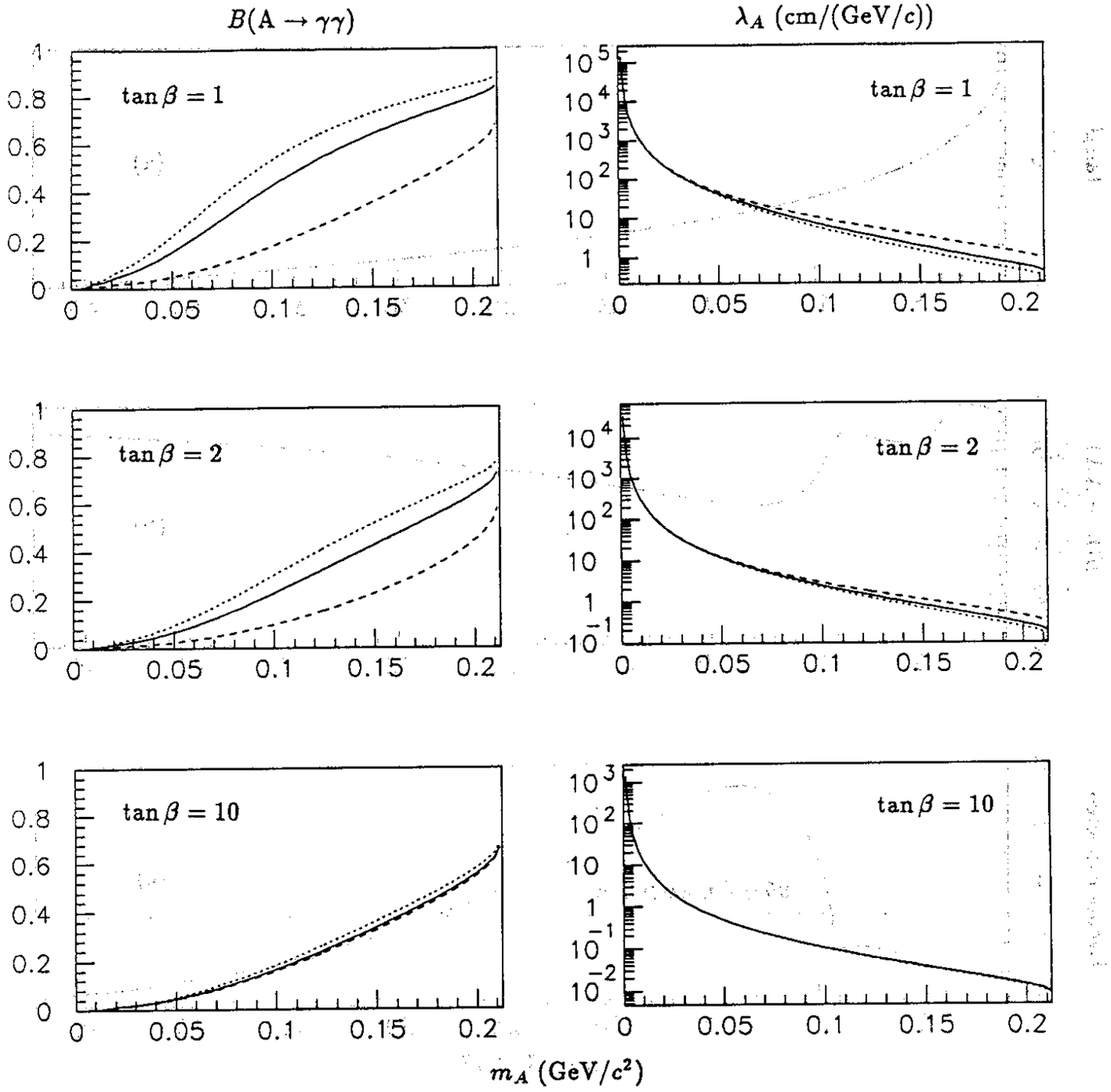
$B(\mathrm{A} \to \gamma\gamma)$
λ_A (cm/(GeV/c))
$\tan\beta = 1$
$\tan\beta = 2$
$\tan\beta = 10$
m_A (GeV/c^2)

Figure 1

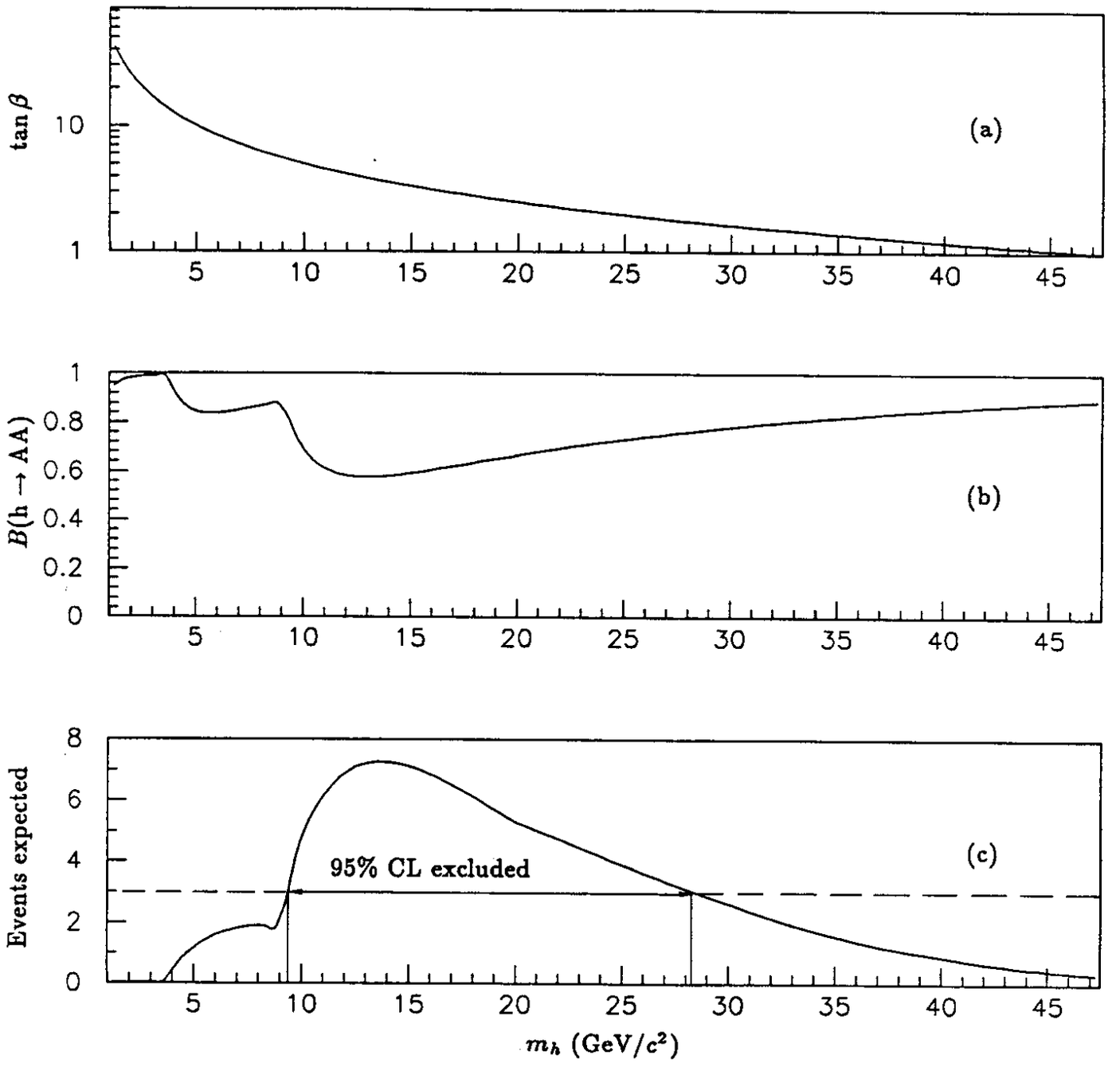
tan β
10
1
(a)
5
10
15
20
25
30
35
40
45
B(h → AA)
1
0.8
0.6
0.4
0.2
0
(b)
Events expected
8
6
4
2
0
95% CL excluded
(c)
m_h (GeV/c²)

Figure 2

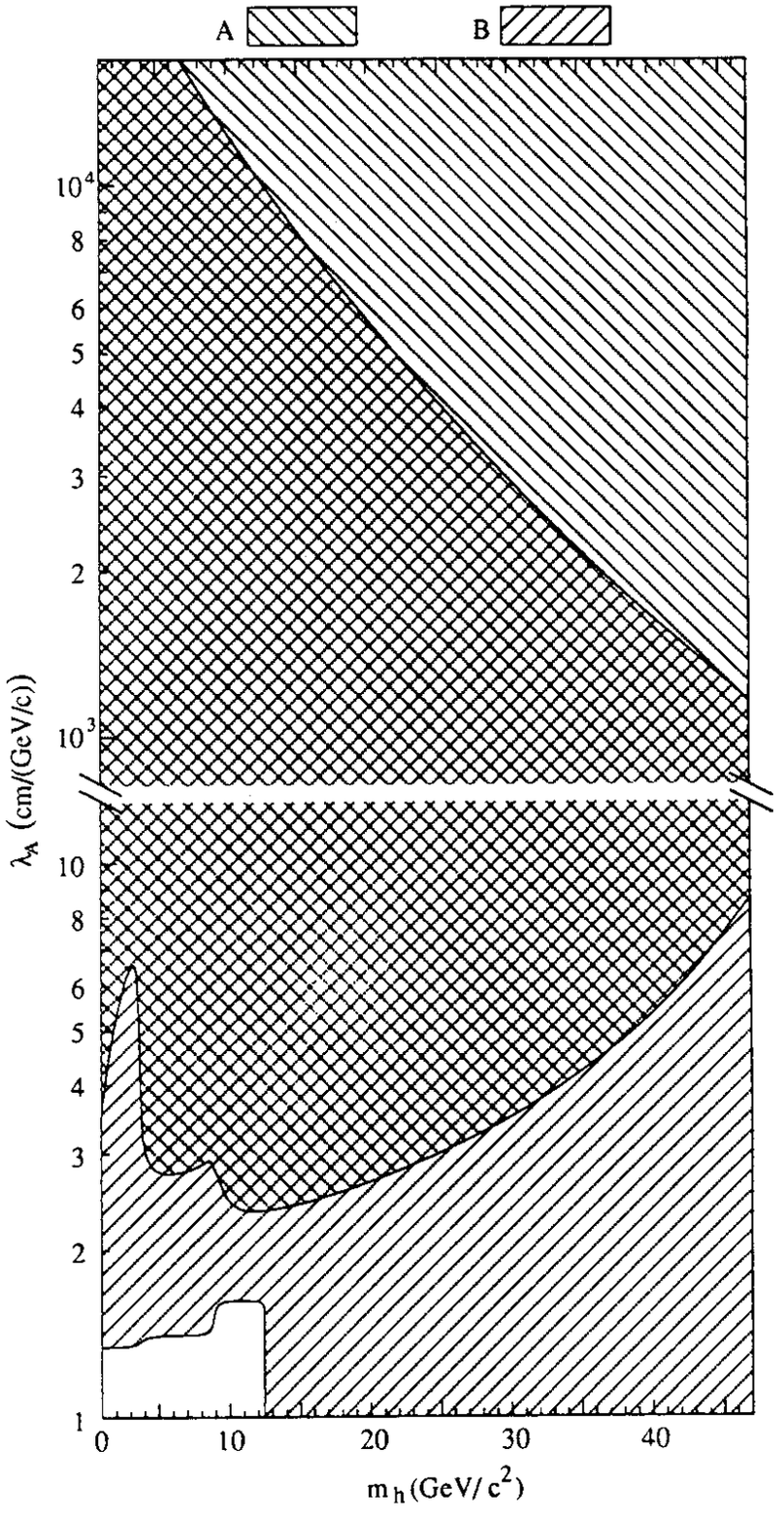
A
B
10^4
8
6
5
4
3
2
10^3
10
8
6
5
4
3
2
1
λ_A (cm/(GeV/c))
0
10
20
30
40
m_h(GeV/c^2)

Figure 3

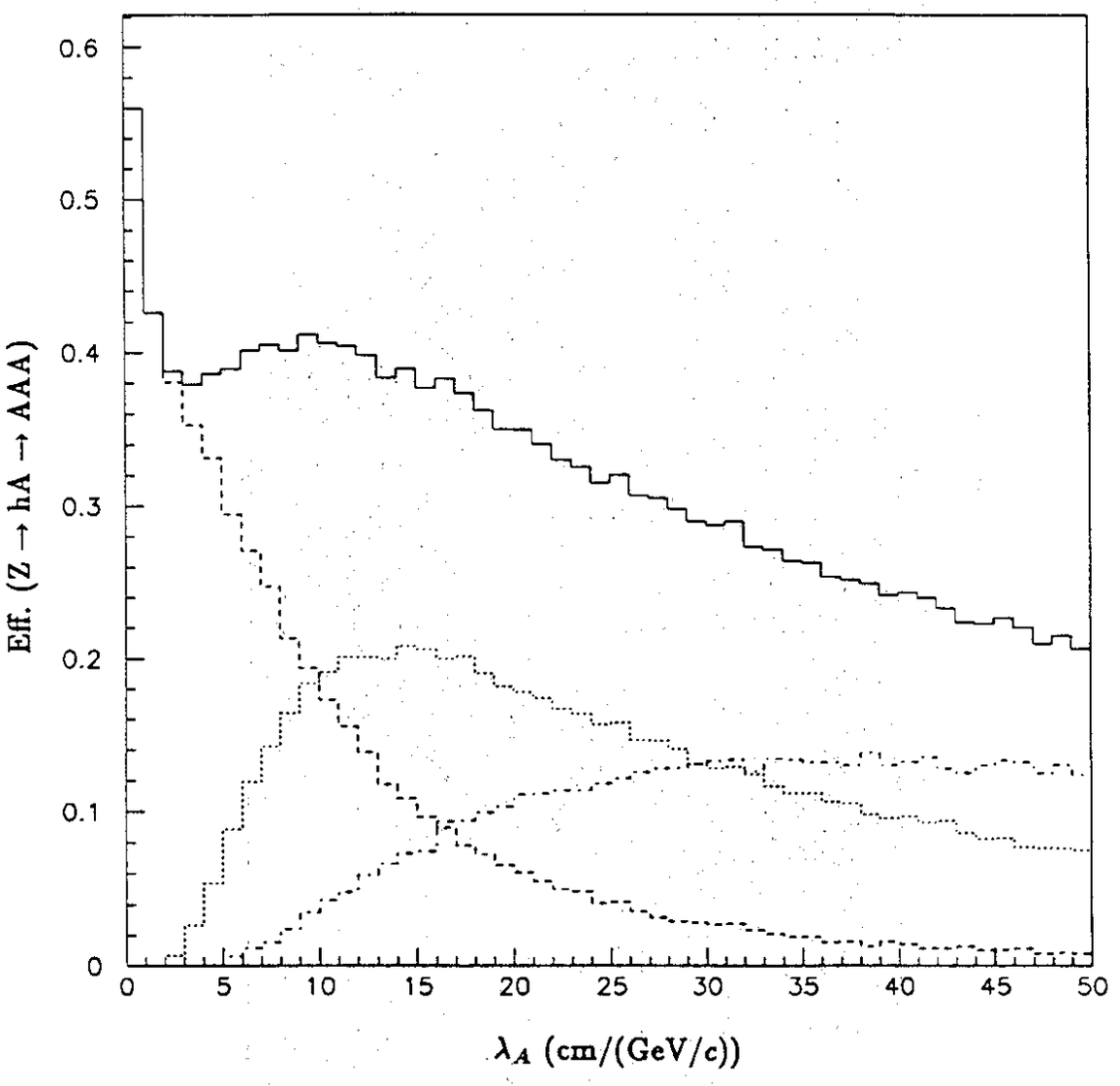
0.6
0.5
0.4
0.3
0.2
0.1
0
Eff. (Z → hA → AAA)
0
5
10
15
20
25
30
35
40
45
50
λ_A (cm/(GeV/c))

Figure 4

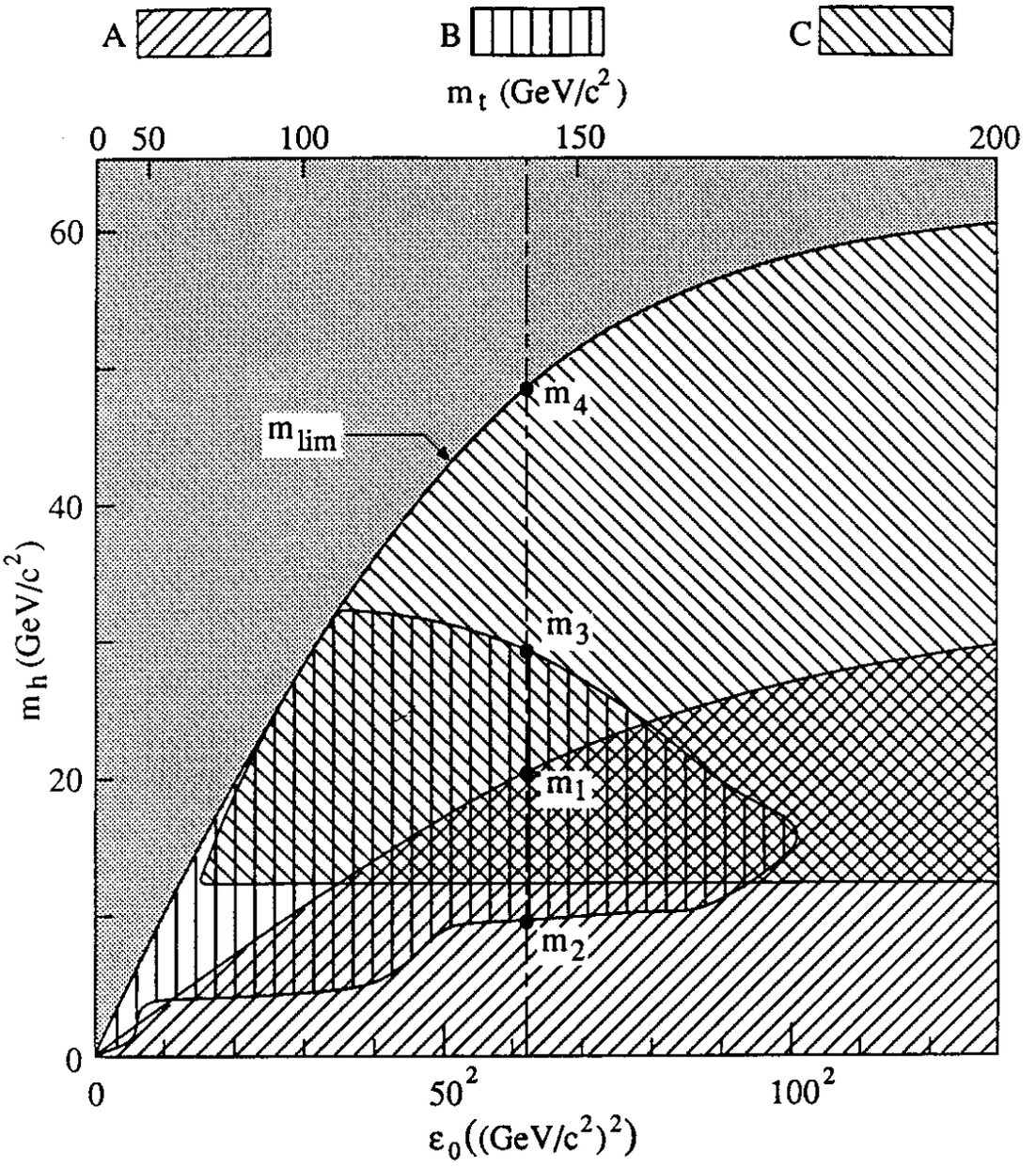
A
B
C
m_t (GeV/c^2)
0
50
100
150
200
60
40
20
0
m_h (GeV/c^2)
m_{lim}
m_4
m_3
m_1
m_2
0
50^2
100^2
ε_0((GeV/c^2)^2)

Figure 5